Aerothermodynamic Heating and Performance Analysis of a High-Lift Aeromaneuvering AOTV Concept

Gene P. Menees* and Kevin G. Brown†
NASA Ames Research Center, Moffett Field, California
and
John F. Wilson‡ and Carol B. Davies‡
Sterling Software, Palo Alto, California

The thermal-control requirements for design-optimized aeromaneuvering performance are determined for space-based applications and low Earth orbit sorties involving large, multiple plane-inclination changes. The leading-edge heating analysis for hypersonic-rarefied flow over lifting surfaces at incidence includes the effects of leading-edge bluntness, low-density viscous phenomena, and finite-rate flowfield chemistry and surface catalysis. The predicted aerothermodynamic heating characteristics are correlated with thermal-control and flight-performance capabilities. The mission payload capability for delivery, retrieval, and combined operations is determined for round-trip sorties extending to polar orbits. Recommendations are given for future design refinements. The results help to identify technology issues required to develop prototype operational systems.

Nomenclature

AOTV = aeroassisted orbital-transfer vehicle
C_D = drag coefficient (function of H and α)
CFD = computational fluid dynamics
GEO = geosynchronous orbit
H = altitude
i = plane-inclination angle from equatorial plane
L/D = lift-drag ratio (function of H and α)
LEO = low Earth orbit
$\dot{q}$ = convective heat flux
Q = total heat load over flight trajectory
t = flight time from $H = 150$ km
V_∞ = flight velocity
x,y,z = Cartesian coordinates referenced to centerline and tip of forecone of basic biconic
α = angle of attack
β = ballistic coefficient (function of H and α)
Δi = change in orbital inclination from Shuttle orbit ($i = 28.5$ deg)
ΔV = propulsive thrust velocity increment
γ = flight-path angle relative to local horizon
ϕ = bank angle (lateral orientation of lift-plane vector relative to Earth-surface normal vector; e.g., $\phi = 0$ deg straight up, $\phi = 180$ deg straight down)

Subscripts

le = leading edge
s = stagnation point
e = entry flight-path angle from $H = 150$ km
f = exit flight-path angle from $H = 150$ km
g = glide-path angle

Presented as Paper 85-1060 at the AIAA 20th Thermophysics Conference, Williamsburg, VA, June 19-21, 1985; received Jan. 3, 1986; revision submitted June 11, 1986.

*Research Scientist. Associate Fellow AIAA.
†Captain, U.S. Air Force. Member AIAA.
‡Consultant, Professional Services Operations West.

Introduction

RECENT exploratory studies have shown that two classes of aeroassisted orbital-transfer vehicles (AOTV) can satisfy the bulk of the nation's future Earth-centered, space-transport missions.[1] One design is useful primarily as a space freighter for transporting large payloads when time is not a constraint in the mission requirements. This aerobraking vehicle performs its orbital-change maneuvers by aerodynamic drag in the far outer extent of the atmosphere to alleviate surface heat fluxes and pressure forces, which minimizes weight penalties for the aeroassist apparatus. An extensive design and mission-performance analysis for operations encompassing cislunar space was given previously for an AOTV concept in this category.[2-4] Similar designs have also been proposed but with somewhat reduced scope in the mission analysis (e.g., Ref. 5). The other generic AOTV design is a very high-lift aeromaneuvering vehicle. This is an essential operational requirement if time-constrained, aeroassisted maneuvers are to be made between low Earth orbits (LEO) involving large, multiple plane-inclination changes. Such high-lift vehicles serve as space taxis. They achieve rapid response from one orbital plane to another, but have the inherent liability of small payload fraction because of low-volumetric efficiency. More advanced versions of this design would have the capability to descend through the atmosphere and land at designated locations on Earth. Results were presented previously[4] of an initial analysis which defined the aerodynamic characteristics, aerothermodynamic heating, and thermal-protection system requirements for a proposed configuration in the high-lift category. This work was the first to address the problem of rarefied-hypersonic flow over a lifting surface at incidence with the inclusion of appropriate viscous/inviscid interaction phenomena.

The purpose of the present study is to extend the previous work to obtain greater depth in the feasibility analysis of the proposed high-lift AOTV design. In general, contemporary research efforts have concentrated on the aerobraking type of AOTV concept; consequently, the current work is probably the most extensive in the nation for the very important high-lift category. Special attention is being given to refining the aerothermodynamic surface—heating predictions and correlating the results with thermal-protection materials and techniques for reusable space-based applications. Greater detail is obtained in the effects of real-gas, hypervelocity-

rarefied, flow phenomena on finite-rate surface catalysis. This problem has not been completely analyzed previously. The present work is a critical advancement, since convective heating is the dominant surface-heating mechanism and the thermal-protection determinant of the aeromaneuvering class of vehicles. These results are essential to accurately define the altitude range of the operational flight envelope that satisfies proposed missions in near-Earth space.

Flow Phenomenology

The principal features of the shock-layer physics that characterize aeromaneuvering AOTVs are illustrated in Fig. 1. Bow-shock waves are shallow and relatively weak, since designs are by necessity slender to obtain high lift drag ratios (L/D). Flow regimes are hypervelocity and low in density, with entry velocities that are typically of the order of 10 km/s. These conditions produce flowfield temperatures that are sufficiently high to dissociate and ionize air species, but below the level for significant radiation transport. However, nonequilibrium relaxation phenomena may have important consequences to the shock-layer thermochemistry and transport properties. Molecular diffusion and finite-rate chemical reactions have a large variation in the rarefied-AOTV flight regimes. This variation can significantly affect surface catalysis and convective heating, which is especially important since convection is the dominant surface-heating mechanism. For the more advanced ground-based versions of the aeromaneuvering AOTV, turbulent-boundary-layer transition criteria and hypersonic viscous/inviscid interaction effects become important factors in the flowfield analysis. However, the present study is concerned with only the space-based design; analysis based on Shuttle flight data indicates that laminar flow conditions prevail over the flight regimes considered herein.

Vehicle Design

The basic geometry of the present high-lift aeromaneuvering configuration is shown in Fig. 2. The design is completed by the addition of a transport complex to the upper surface that contains components for the propulsion system, command and control capsule (including avionics and reaction-control system motors for attitude control), and cargo module. The vehicle is approximately 35 m in length, which is necessary to accommodate the rocket engines and obtain the high-lift requirements for large payloads. The shape is derived from hypersonic lifting-body theory using truncated biconics with smoothing through the juncture point between the fore and aft cones to eliminate the discontinuity. The design avoids the complex shock-interaction effects of winged configurations, which cause highly localized heat fluxes and severe thermal-control requirements. The aerodynamic characteristics are optimized in parametric studies by varying the angles of the fore and aft cones, the bend angle between the cones, and the upper-surface curvature, which is truncated with second-order polynomials. The results have been compared with traditional hypersonic lifting configurations (e.g., delta wings and truncated cones) and the advantages that provide design superiority identified. Principal among these advantages are the sharp leading edges, which are beneficial in maintaining high lift in rarefied-hypersonic-flow flight regimes, and the variable static margin, which provides longitudinal stability and self-trimming capability over a broad angle-of-attack range. Complete details of the optimization procedure for the aerodynamic and vehicle-systems designs are given in a companion paper.[6]

Results and Discussion

Aerodynamic Characteristics

Crucial to the success of the design of an aeromaneuvering AOTV is the achievement of the maximum-possible lifting capability, which is specified by L/D. This capability determines the lateral-turn performance to obtain plane-inclination changes with minimal propulsion energy, within the altitude constraints imposed by aerothermodynamic heating and thermal-protection limitations. A comparison of the viscous and inviscid lifting characteritics of the present vehicle is shown in Fig. 3 for typical flight conditions and the operational incidence that accommodates the transport complex.[6] These results include the effects of leading-edge bluntness, which is considered necessary because of the reusable, space-based operational requirements. Depending on the materials used to construct the sharp leading edges, gradual blunting or rounding may occur because of the heating effects of repeated flights. Complete details of the calculations are given in Ref. 6. In general, it was found that leading-edge radii of the order

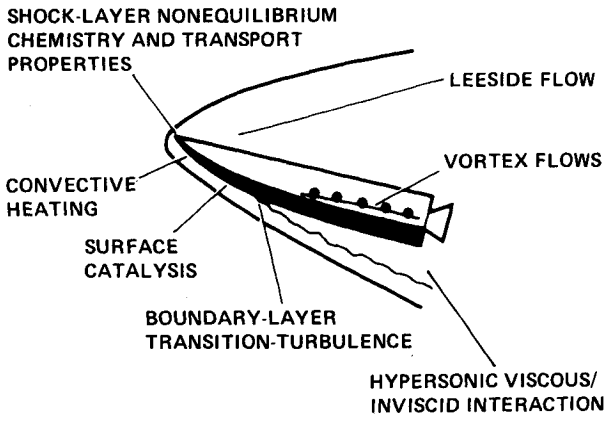

Fig. 1 Hypervelocity flowfield phenomenology of high-lift aeromaneuvering sortie vehicle.

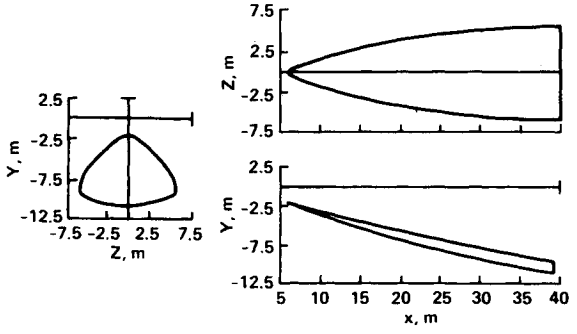

(a) TWO DIMENSIONAL

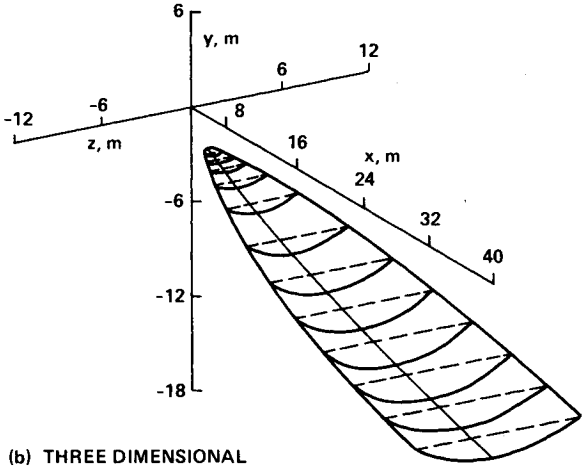

(b) THREE DIMENSIONAL

Fig. 2 Geometry of high-lift aeromaneuvering truncated, bent-biconic AOTV concept (fore-cone half angle = 20 deg, aft-cone half angle = 8 deg, bend angle = 2 deg; from Ref. 6).

of 10 cm could be accommodated without serious degradation of the aerodynamic characteristics. The inviscid results were determined from hypersonic Newtonian theory. Corrections for low-density viscous effects were then applied using the momentum equation for the two-dimensional boundary layer as a basis to account for surface curvature effects. The phenomena characteristic of rarefied-hypersonic flow over a flat plate (i.e., free-molecular flow at the leading edge that evolves downstream through a transition region and merged layer before attaining the classical boundary-layer flow with weak-interaction effects) were used to generate the equations describing the boundary-layer growth rate. The skin-friction forces at each point of the body surface were accounted for in determining the aerodynamic characteristics.

The results are correlated in Fig. 3 as a function of altitude and vividly dramatize the strong deterioration of lifting capability resulting from the low-density viscous effects. The rapid inverse decay of L/D with H is nearly 50% between 70- and 90-km altitude. This effect significantly decreases the lateral-turn performance, which is directly proportional to L/D. Consequently, it is desirable to operate the vehicle at the lowest possible altitude flight regime to provide the high L/D that optimizes the plane-change procedure and payload capacity. However, the major constraint is the altitude limitation on the aerothermodynamic heating imposed by contemporary thermal-control and materials technology for space-based applications, as will be discussed subsequently.

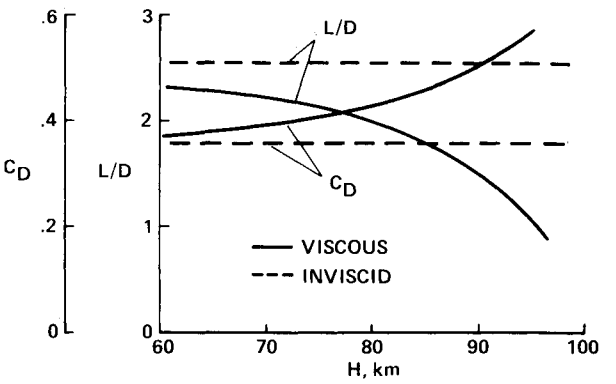

Fig. 3 Typical aerodynamic characteristics ($V_e = 10.3$ km/s, $\alpha = 6.5$ deg).

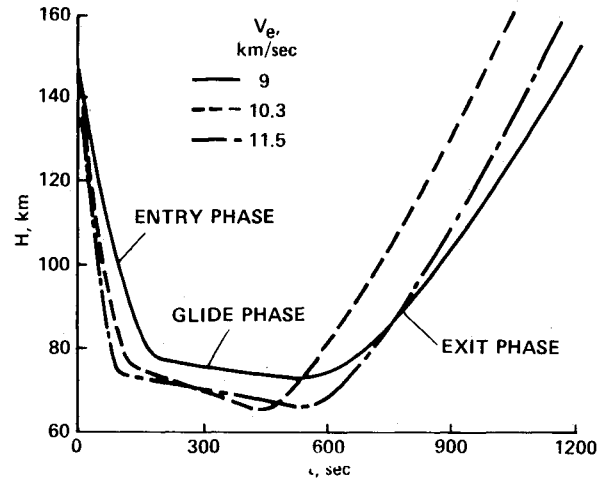

Fig. 4 Flight trajectories for various entry conditions and optimal orbital transfer to target LEO.

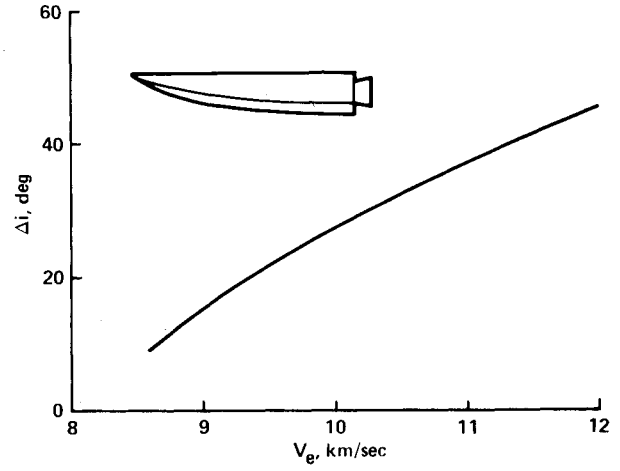

Fig. 5 Plane-inclination change capability as a function of entry velocity.

Trajectory Analysis

The principal flight parameters (V, γ, ϕ) were varied in parametric comparative studies to determine the relative tradeoffs between plane-change capability and the corresponding aerothermodynamic heating requirements. The objective was to maintain the highest possible altitude to minimize the surface heating, yet still obtain substantial aeroturning (Δi) and the necessary aerobraking for optimal transfer to the target LEO. Only aerodynamic transatmospheric maneuvers are considered in this study. (The synergetic maneuver, or simultaneous application of propulsive thrust, will be analyzed in future work.) The flight strategy employed during the atmospheric pass consists of three phases: 1) the entry phase in which V_e, γ_e, and ϕ_e are selected to achieve a trajectory perigee that provides the desired compromise in Δi and $\dot{q}_s$ ($\phi_e = 90$ deg); 2) the glide phase in which γ_g and ϕ_g are held nearly constant to maintain high altitude ($\phi_g \approx 180$ deg to produce negative lift, an aerodynamic strategy previously proposed[3] to minimize surface heating and aerodynamic forces); and 3) the exit phase in which γ_f and ϕ_f are selected for maximum lateral turning ($\phi_f = 90$ deg) and optimal orbital transfer with minimal propulsion energy. Two iterations on γ are required in the overall procedure. The first is at the transition from the entry to glide phases at the altitude where a force balance occurs, and the second at the transition from the glide to exit phases where V_e is selected for tangential circularization at the target LEO. Representative results are given in Fig. 4 for entry velocities ranging from 9 to 11.5 km/s. Extending V_e beyond this range produces marginal tradeoffs for Δ_i and $\dot{q}_s$. The corresponding aeroturning or plane-inclination change characteristics of the vehicle are shown in Fig. 5. For GEO-return entry conditions ($V_e \approx 10.3$ km/s), generally a standard comparative base, Δi is about 32 deg, which provides a substantial capability.

Mission Performance Analysis

An essential aspect of this work is a detailed analysis of the proposed high-lift AOTV's ability to satisfy specified mission requirements for payload delivery, retrieval, and combined delivery/retrieval operations. Studies were conducted for a broad range of LEO sortie missions extending to polar orbits. Both the base and target orbits had fixed altitudes of 400 km, with the inclination of the base orbit being equivalent to that of the Shuttle orbit (28.5 deg). This procedure is considered to be an average of proposed LEO sortie operations that involve both multiple-plane and moderate-altitude orbital changes. Altitude differences of approximately 10^4 km can be accommodated by small changes in the aeroassist maneuver without significant propellant penalties. This difference occurs because the high velocity of the vehicle and exponential density variation in the atmosphere significantly change the deceleration characteristics during the transatmospheric pass. The calculations were made using the vehicle-weight specifica-

tions given in Table 1, the full details of which were given previously.[3] For space-based operations, it is proposed to deploy the vehicle, without propellant, in several sections and assemble the components in space. Because of the high circular velocities of LEOs and the limitations of the vehicle's L/D characteristics, a propulsive strategy involving three burns is used as an adjunct to aerodynamic lift to enhance orbital-change maneuvers. This technique is illustrated in Fig. 6 and basically involves transfer orbits of high eccentricity and apogee. Part of the plane change is accomplished propulsively at a much greater altitude than the target LEO, with low expenditure of propellant because of the reduced circular velocity.

The payload capacity for round-trip sorties involving plane changes (i) of about 60, 75, an d90 deg (i.e., $\Delta i = 31$, 45, and 61.5 deg) is illustrated in Figs. 7a, b, and c, respectively. The analysis is based on the plane-change capability for $V_e = 10.3$ km/s and the normal-growth technology of liquid rocket engines having a specific impulse of 480 s. Generous allowances are included for propellant losses resulting from guidance-navigation-control corrections, docking maneuvers, and boil off over the duration of the mission. The optimum orbital-change maneuver is to achieve all of the specified plane changes aerodynamically by direct decircularization from the base LEO. However, this maneuver is generally impractical because of the reduced aerodynamic-lift capability imposed by the relatively low-entry velocity. The various orbital-change strategies that are compared in the present study are listed in Table 2. The all-propulsive direct maneuver of Case 1 cannot achieve any payload capability. Employing the three-impulse, propulsive-thrust maneuver with the transfer-orbit apogee at GEO provides moderate payload capability for $\Delta i = 31$ deg and small payload capability for $\Delta i = 45$ deg. The application of the vehicle's aeromaneuvering capability in combination with the three-impulse-thrust maneuver produces dramatic increases and is the only method that achieves payload for the polar orbit. However, Cases 2 and 3 require sacrifices in the mission duration. The time for the roundtrip scenario is about 21 h, since the GEO distance is traversed twice. If rapid response, time-constrained requirements are a factor, then the direct maneuver of Case 4 provides the best alternative for payload capability. This maneuver requires raising the entry velocity to the equivalent GEO-return value by a propulsive boost performed in conjunction with the GEO-decircularization burn. For the polar mission, it may also be possible to achieve payload by the synergistic technique or flight trajectories that plunge deeper into the lower atmosphere to increase

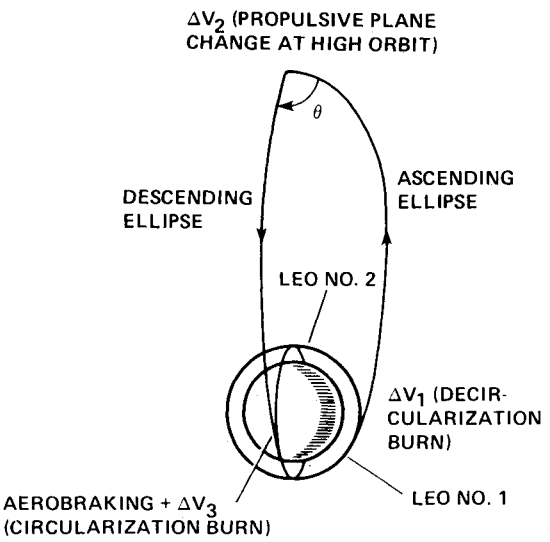

Fig. 6 Three-impulse, propulsive-thrust strategy to minimize propellant usage for sorties between LEOs requiring large plane changes.

Table 1 Vehicle specifications for mission performance analysis

Gross (zero-payload) weight	23,822 kg
Nominal fuel weight (97% of total; i.e., 3% reserves)	18,480 kg
Total allowed lift-off weight (gross weight + payload)	29,484 kg
Dry weight of disposable external tank	1000 kg
Maximum fuel weight in disposable tank	4662 kg

Table 2 Orbital change strategies for payload calculations involving sorties between LEOs with large multiple plane-inclination changes (480-s, specific-impulse rocket engine)

Case 1	All propulsive direct maneuver from base to target LEO.
Case 2	All propulsive maneuver using three-impulse thrust method for low eccentricity transfer orbit with apogee at GEO (21-h roundtrip duration).
Case 3	Combination aerodynamic and three-impulse thrust maneuver with Δi required in excess of aeromaneuvering capability achieved propulsively at apogee of GEO transfer orbit (21-h roundtrip duration).
Case 4	Combination aerodynamic and propulsive direct maneuver by boosting down from LEO on equivalent GEO descent ellipse.

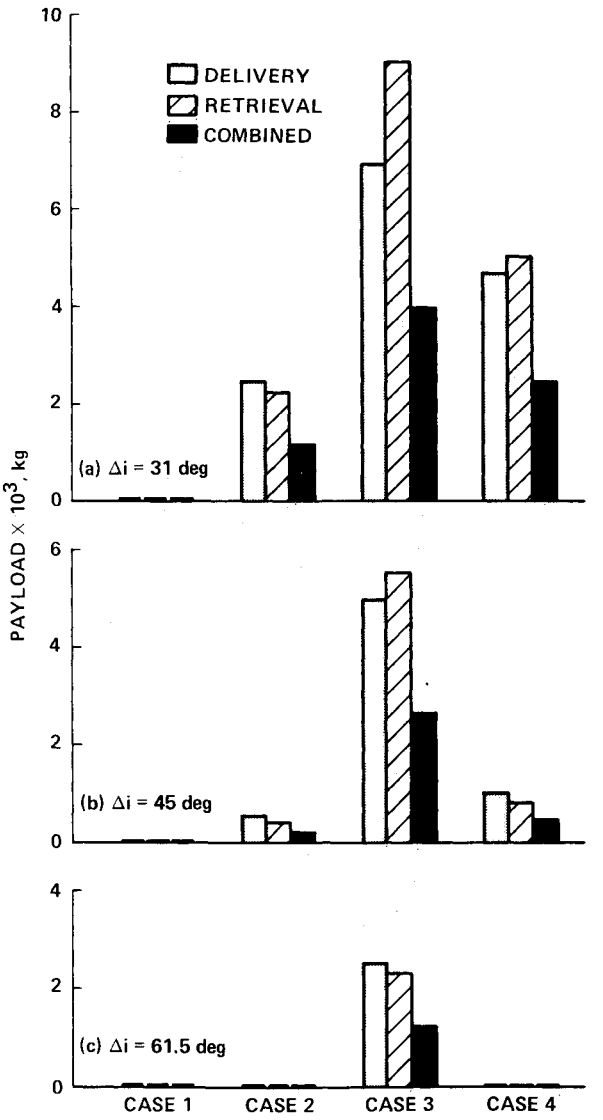

Fig. 7 Maximum payload capability for delivery, retrieval, and combined delivery/retrieval roundtrip sortie missions from LEO at $H = 400$ km.

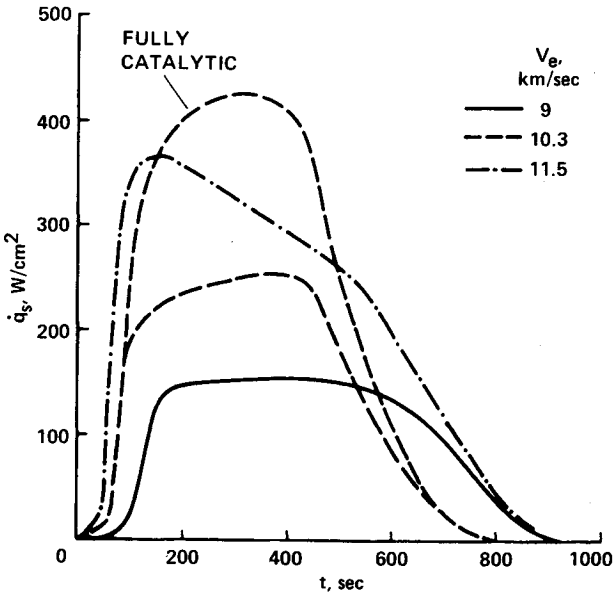

Fig. 8 Stagnation-point heat-flux distributions over flight trajectories (vehicle centerline).

the aerodynamic lift and plane-change capability. However, these methods must be compromised by increased aerothermodynamic-heating requirements.

Aerothermodynamic Heating

The reusable, space-based, operational requirements of the vehicle will ensure the development of some finite leading-edge bluntness after repeated flights. The design optimization studies[6] indicate that leading-edge radii of the order of 10 cm can be accommodated without significant degradation of the aerodynamic-lifting capability. This result motivated the development of a new CFD code[7] that predicts the convective heating to leading edges of small radii in the highly energetic, rarefied-flow flight regimes that characterize aeromaneuvering AOTVs. These conditions produce unique flow phenomena that have not been completely analyzed previously. The principal ones are increased shock and boundary-layer thicknesses that merge into a "viscous layer" and finite-rate relaxation effects, since the post-shock flow is in a state of thermochemical nonequilibrium.[8] In addition, the traditional Rankine-Hugoniot shock-jump relations become invalid and must be modified to account for the viscous transport, or "shock-slip" conditions.[9,10] The new viscous-shock-layer code[7] advances the previous work by including coupled vibrational nonequilibrium effects into the analysis, but currently excludes ionization phenomena. The code is based on the thin shock-layer form of the boundary-layer equations for stagnation-point flow.[11] Although developed from continuum theory, this approach provides good results up to the free-molecular limit, with the low-density effects properly accounted for.

The present analysis uses the ideal dissociating-gas model of air[12] for the chemical kinetic processes, which has been shown previously to give good heat-transfer results.[11,13] Properties are based on the mass-weighted average of a mixture consisting of 79% nitrogen and 21% oxygen by volume. A constant Prandtl number (0.71), Lewis number (1.0), and pressure are assumed across the shock layer. The ratio of specific heats is fixed at 9/7, and the viscosity is assumed to be proportional to the three-fourth power of temperature. The dissociation-recombination model is that of Kang,[14] and the reaction-rate coefficients are those of Park.[10] The catalyticity of the surface material is assumed to be similar to that of the Shuttle, and the wall recombination-rate parameter is calculated from the data of Scott.[15]

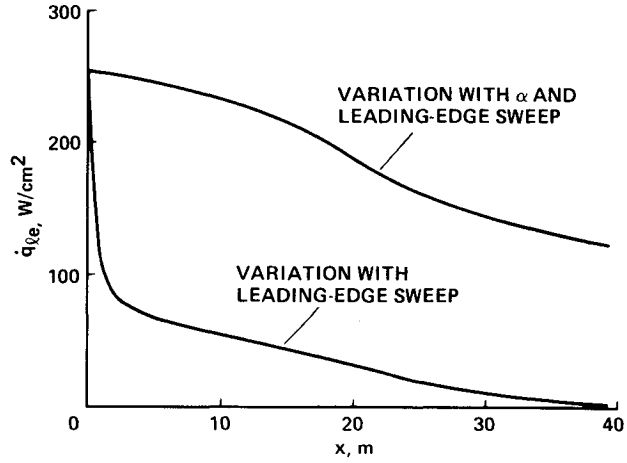

Fig. 9 Leading-edge, heat-flux distributions at peak heating point in $V_e = 10.3$ km/s trajectory (plotted at corresponding x location on vehicle centerline).

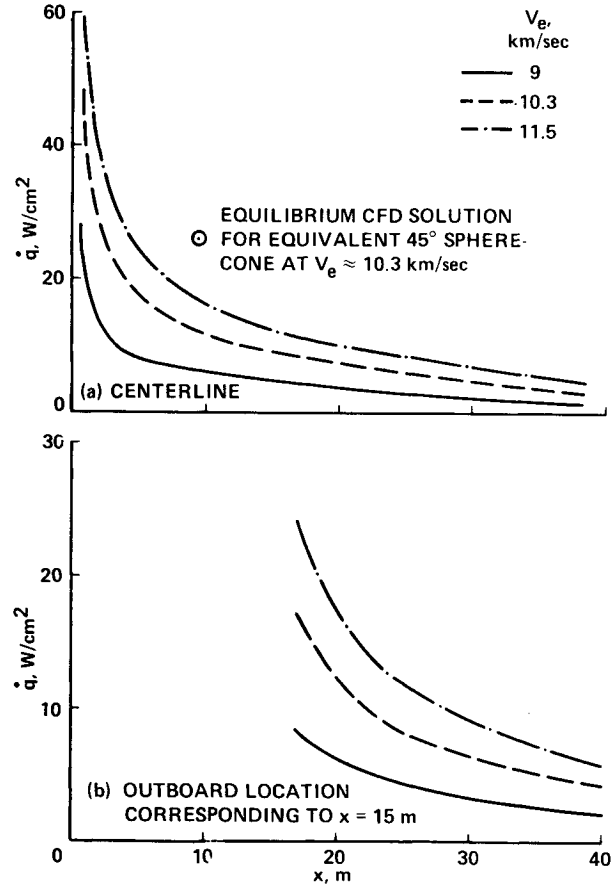

Fig. 10 Streamwise heat-transfer distributions at peak heating point in flight trajectories.

The predicted distributions of the stagnation-point heat fluxes at the vehicle tip (centerline) are shown in Fig. 8 over the various flight trajectories. The calculations are based on a leading-edge radius of 10 cm and a surface temperature of 1500 K. The value of the wall-rate parameter corresponding to this temperature is about 5.7 m/s. Its effect on the surface heat-transfer rate is demonstrated in Fig. 8 for the $V_e = 10.3$ km/s trajectory, where the fully catalytic case is also shown and can be compared with the finite-rate result. More than a 40% reduction in surface heating is produced by the low catalyticity of the Shuttle-type ceramic material. The magnitude of the heat flux is a strong function of the entry

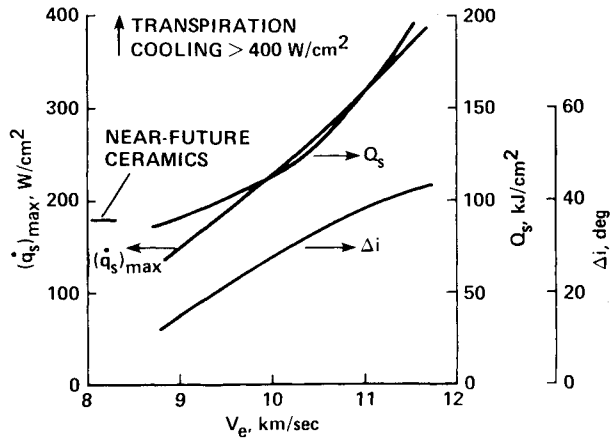

Fig. 11 Summary of surface-heating requirements and correlation with thermal-control capabilities.

velocity, with about a factor of 3 difference between the high and low values of V_e. Interestingly, there is also about a factor of 3 difference in the plane-change achieved for these two cases (see Fig. 5). Consequently, a serious penalty in Δi is obtained as the price for significant reductions in $\dot{q}_s$.

Results that are typical of the heat-flux distribution around the leading edge of the vehicle are shown in Fig. 9 for the peak-heating point in the $V_e = 10.3$ km/s trajectory. Two cases are given which include the variation for both angle of attack and leading-edge sweep and for leading-edge sweep only. The stagnation-point heat-transfer calculations were obtained for hemispherical blunting of the vehicle tip, with the assumption that incidence effects were negligible. The swept-back leading edges, however, more closely approximate circular cylinders that are oblique to the flow, and neglecting incidence effects may be invalid. The results shown represent approximate upper and lower limits.

Representative streamwise distributions of the surface-heat flux on the windward surface are shown in Fig. 10 for the three flight trajectories analyzed. The results correspond to the peak-heating points at two locations on the vehicle surface: the centerline (Fig. 10a) and an outboard location at $x = 15$ m (Fig. 10b and Fig. 2). The calculations were obtained using the weak-interaction effects formulation,[16,17] corrected for incidence, as being the most appropriate downstream match to the blunt leading-edge flow. The overall result is that the magnitude of $\dot{q}$ decreases very rapidly from the leading edge and is less than 20 W/cm^2 over most of the vehicle surface. Also shown in Fig. 10a is a predicted CFD, fully coupled, equilibrium solution for an equivalent 45 deg-sphere cone and $V_e \approx 10.3$ km/s.[1] The difference between this result and the present solution is about a factor of 2, which is reasonable considering the physics involved. The CFD solution is axisymmetric and three dimensional, whereas, the present flat-plate solution is two-dimensional. This difference produces strong, viscous, crossflow effects that increase the surface heating. Furthermore, the incidence angles for the two solutions differ (i.e., 45 deg for the CFD and about 30 deg for the present analysis), which causes additional increases that can easily account for the overall difference in the predictions.

Thermal Control

The essential surface-heating requirements are summarized in Fig. 11 and correlated with aeromaneuvering plane-change and thermal-control capabilities. The limitation invoked by the near-future development of high-temperature reusable materials[4,18] (i.e., ceramics with about 2-years lead time) corresponds to a $\dot{q}_s$ of approximately 180 W/cm^2, or a surface temperature of about 2500 K for equilibrium radiative emission of all the absorbed heat. This limitation constrains the aeroturning capability to $\Delta i \approx 20$ deg at $V_e \approx 9.4$ km/s. The Q_s for these conditions is about the same as that for the Galileo probe (100 kJ/cm^2). However, the reduction in Q_s caused by conduction and radiative emission is not considered in these results, but may be substantial because of the long duration of the flight time. Heat loads of this magnitude require ablating-type thermal-protection materials. The previous results[4] also showed that severe heat transfer occurs only within small localized areas near the leading edge. As a consequence, it may be possible to replace the affected regions with new material between missions. If the replacement proves impractical, the heat-rejection characteristics may be improved dramatically by using the heat capacity of the propulsion fuel, or other liquids, to cool the spacecraft skin in either forced or transpiration methods. For example, an active cooling system, transpiration-cooled with water, has been proposed[19] that protects a reusable all-metal spacecraft flying a hot re-entry corridor with descent from GEO. Calculated skin temperatures range above 4000 K for the stagnation point to nearly 1400 K on the underside. This technique achieves without difficulty the $\Delta i = 31$ deg for V_e corresponding to GEO return, and may make possible a Δi as much as 45 deg for $V_e = 12$ km/s. There are serious compromises to consider for the payload sacrificed as a result of the volume and weight penalties necessary to implement active cooling requirements. However, a moderate payload capacity is generally acceptable for the specialized objectives of rapid-response, time-constrained missions.

Concluding Remarks

A study has been conducted that establishes the approximate aerothermodynamic heating and thermal-control requirements of a proposed high-lift AOTV design for LEO sortie missions involving large-multiple, plane-inclination changes. The aerodynamic characteristics are the first to account for hypervelocity, low-density, viscous phenomena. The surface heating predictions advance previous work by including vibrational nonequilibrium effects on both the flow field and surface catalysis.

The flight strategy used for the aeroassist maneuver is designed to achieve an acceptable compromise between the surface-heating characteristics and aeromaneuvering capability. Severe heat transfer, beyond the range of contemporary reusable thermal-protection materials, occurs only in highly localized regions around the leading edge. However, total heat loads are substantial because of the long duration of the atmospheric transits. Ablating materials or active-cooling techniques are required to accommodate the heating requirements necessary to achieve significant plane-inclination changes; e.g., transpiration cooling may make possible aeromaneuvering plane changes as great as 45 deg. The mission performance with realistic aeromaneuvering capability for payload delivery and retrieval is demonstrated for LEO sorties extending to polar orbits. Substantial capacity is obtained for all scenarios with proper application of the three-impulse, propulsive-thrust orbital-change maneuver. No payload is currently possible for rapid-response, time-constrained polar missions; however, improved lifting capability obtained by reducing the vehicle's transport complex requirements may achieve some small payload delivery. In addition, further study of alternate flight strategies may produce beneficial tradeoffs between the aeromaneuvering characteristics and thermal-control requirements that provide increased performance capability.

Future design optimization requires advancements in the aerodynamic/aerothermodynamic prediction methods that account for rarefaction phenomena and real-gas effects. A multidimensional CFD code must incorporate these features, since the three-dimensional surface contour produces nontrivial effects. In addition, there are important thermochemical problems that must be addressed. Principal among these are nonequilibrium reaction rates and transport

properties, which have a wide but unknown variation in the rarefied-AOTV flight regimes, and signifcantly affect surface catalysis and convective heating.

References

[1]Menees, G. P., "Thermal Protection Requirements for Near-Earth Aeroassisted Orbital Transfer Missions," *Thermal Design of Aeroassisted Orbital Transfer Vehicles*, edited by H. F. Nelson, Vol. 96, *Progress in Astronautics and Aeronautics*, AIAA, New York, 1984, pp. 257-285.

[2]Davis, C. B. and Park, C., "Aerodynamics of Generalized Bent Biconics for Aero-Assisted Orbital-Transfer Vehicles," *Journal of Spacecraft and Rockets*, Vol. 22, March-April 1985, pp. 104-111.

[3]Menees, G. P., Park, C., and Wilson, J. F., "Design and Performance Analysis of a Conical Aerobrake Orbital Transfer Vehicle Concept," *Thermal Design of Aeroassisted Orbital Transfer Vehicles*, edited by H. F. Nelson, Vol. 96, *Progress in Astronautics and Aeronautics*, AIAA, New York, 1984, pp. 286-308.

[4]Menees, G. P., Davies, C. B., Wilson, J. F., and Brown, K. G., "Aerothermodynamic Heating Analysis of Aerobraking and Aeromaneuvering Orbital Transfer Vehicles," *Thermal Design of Aeroassisted Orbital Transfer Vehicles*, edited by H. F. Nelson, Vol. 96, *Progress in Astronautics and Aeronautics*, AIAA, New York, 1984, pp. 338-360.

[5]Scott, C. D., Reid, R. C., Maraia, R. J., Li, C. P., and Derry, S. M., "An AOTV Aeroheating and Thermal Protection Study," *Thermal Design of Aeroassisted Orbital Transfer Vehicles*, edited by H. F. Nelson, Vol. 96, *Progress in Astronautics and Aeronautics*, AIAA, New York, 1984, pp. 309-337.

[6]Davies, C. B. and Park, C., "Optimum Configuration of High-Lift Orbital Transfer Vehicles," AIAA Paper 85-1059, 20th Thermophysics Conference, Williamsburg, VA, June 19-21, 1985.

[7]Brown, K. G., "Chemical and Thermal Nonequilibrium Heat Transfer Analysis for Hypervelocity, Low Reynolds Number Flow," AIAA Paper 1033, 20th Thermophysics Conference, Williamsburg, VA, June 19-21, 1985.

[8]Probstein, R. F. and Kemp, N. H., "Viscous Aerodynamic Characteristics in Hypersonic Rarefied Gas Flow," *Journal of the Aero/Space Sciences*, Vol. 27, March 1960, pp. 174-192.

[9]Cheng, H. K., "Hypersonic Shock-Layer Theory of the Stagnation Region at Low Reynolds Number," *Proceedings of the 1961 Heat Transfer and Fluid Mechanics Institute*, Stanford University Press, Stanford, CA, 1962, pp. 161-175.

[10]Park, C., "Problems of Rate Chemistry in the Flight Regimes of Aero-Assisted Orbital Transfer Vehicles," *Thermal Design of Aeroassisted Orbital Transfer Vehicles*, edited by H. F. Nelson, Vol. 96, *Progress in Astronautics and Aeronautics*, AIAA, New York, 1984, pp. 511-537.

[11]Park, C., "Dissociative Relaxation in Viscous Hypersonic Shock Layers," *AIAA Journal*, Vol. 2, July 1964, pp. 1202-1207.

[12]Lighthill, M. J., "Dynamics of a Dissociating Gas, Part I, Equilibrium Flow," *Journal of Fluid Mechanics*, Vol. 2, Jan. 1957, pp. 1-32.

[13]Chung, P. M., Holt, J. F., and Lin, S. W., "Merged Stagnation Shock Layer of Nonequilibrium Dissociating Gas," *AIAA Journal*, Vol. 6, Dec. 1968, pp. 2372-2379.

[14]Kang, S. W., "Nonequilibrium Ionized Hypersonic Flow Over a Blunt Body at Low Reynolds Number," *AIAA Journal*, Vol. 8, July 1970, pp. 1263-1270.

[15]Scott, C. D., "Effects of Nonequilibrium and Catalysis on Shuttle Heat Transfer," *Journal of Spacecraft and Rockets*, Vol. 22, Sept.-Oct. 1985, pp. 489-499.

[16]Wallace, J. E. and Burke, A. F., "An Experimental Study of Surface and Flow Field Effects in Hypersonic Low Density Flow Over a Flat Plate," *Rarefied Gas Dynamics, Supplement 3*, Vol. 1, 1965, pp. 487-507.

[17]McCroskey, W. J., Bogdonoff, S. M., and McDougall, J. G., "An Experimental Model for the Sharp Flat Plate in Rarefied Hypersonic Flows," *AIAA Journal*, Vol. 4, Sept. 1966, pp. 1580-1587.

[18]Menees, G. P., Park, C., Wilson, J. F., and Brown K. G., "Determination of Atmospheric Density Using a Space-Launched Projectile," *Journal of Spacecraft and Rockets*, Vol. 23, May-June 1986, pp. 273-280.

[19]Salkeld, R., Beichel, R., and Skulsky, R., "A Reusable Space Vehicle for Direct Descent from High Orbits," *Astronautics and Aeronautics*, April 1981, pp. 46-63.